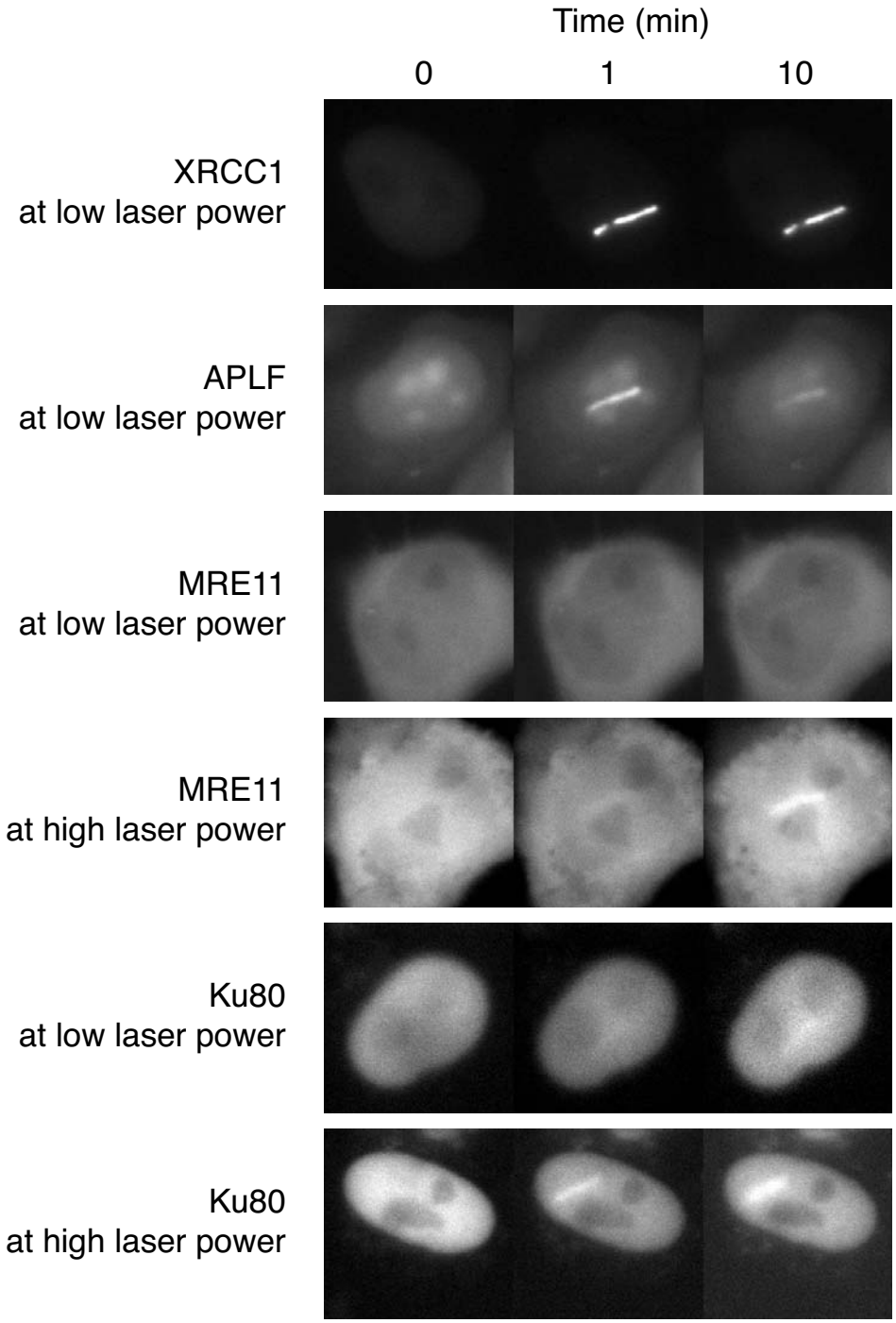

Supplementary Fig. 1 | Recruitment of single- and double-strand DNA break binding proteins to laser microirradiation sites.
The assays reveal that single-strand DNA damage proteins (such as APLF and XRCC1) readily recruit to laser micro-irradiation sites, including at the "low" laser power settings used in this study. In contrast, the double-strand DNA damage proteins MRE11 and Ku80 require "medium" to "high" laser power in order to be seen recruiting to the DNA damage sites. Most laser microirradation experiments in this study were conducted at "low" laser power, suggesting that we are primarily dealing with single DNA-strand-induced PARP1 activation.

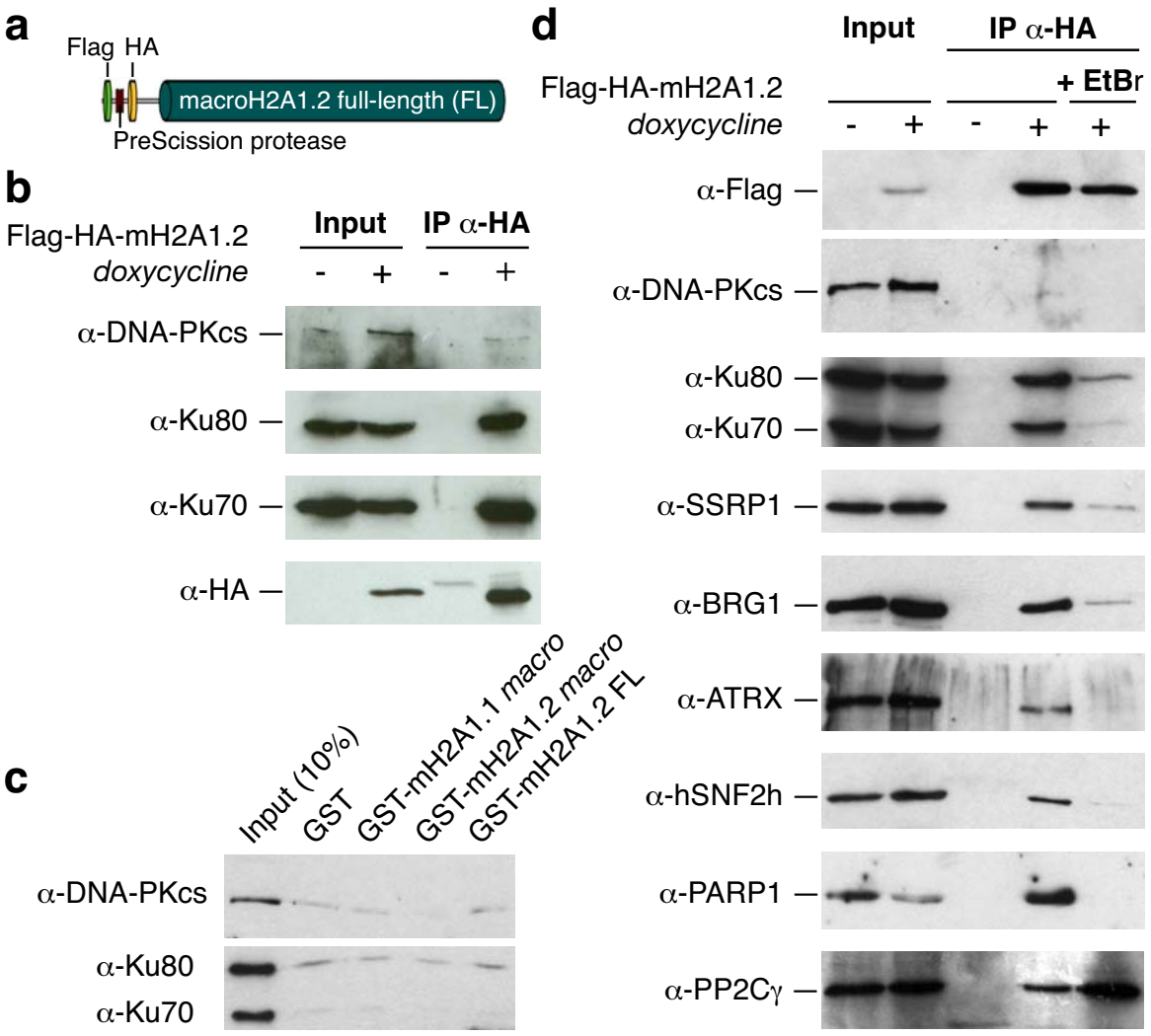

Supplementary Fig. 2 | Purification of proteins associating with full-length histone macroH2A1.2.

a, Monoclonal HeLa cells lines expressing a Flag-PreScissionProtease-HA-tagged macroH2A1.2 transgene under the control of a doxycycline-inducible promoter were generated. **b**, Western blot assays of anti-HA-antibody-mediated co-immunoprecipitation experiments from nuclear extracts confirm DNA-dependent protein kinase, Ku80 and Ku70 as interactors. **c**, GST-pulldown assays between immobilized macrodomains and highly-purified DNA-PK holocomplex (consisting of the catalytic DNA-PK subunit and the Ku70/80 heterodimer). GST proteins consisted of histone macroH2A1.1 macrodomain, macroH2A1.2 macrodomain, full-length macroH2A1.2 and GST-only negative control. Purified holo-DNA-PK fails to associate with full-length macroH2A1.2 or with the macrodomains of macroH2A1.1 and macroH2A1.2. **d**, Western blots of macroH2A1.2-interacting proteins immunopurified by tandem affinity purification with both anti-FLAG and anti-HA antibody in the presence and absence of the DNA intercalator ethidium bromide. Except for protein phosphatase 2Cγ, a known H2A-H2B histone chaperone[30], ethidium bromide strongly reduces all identified interactions.

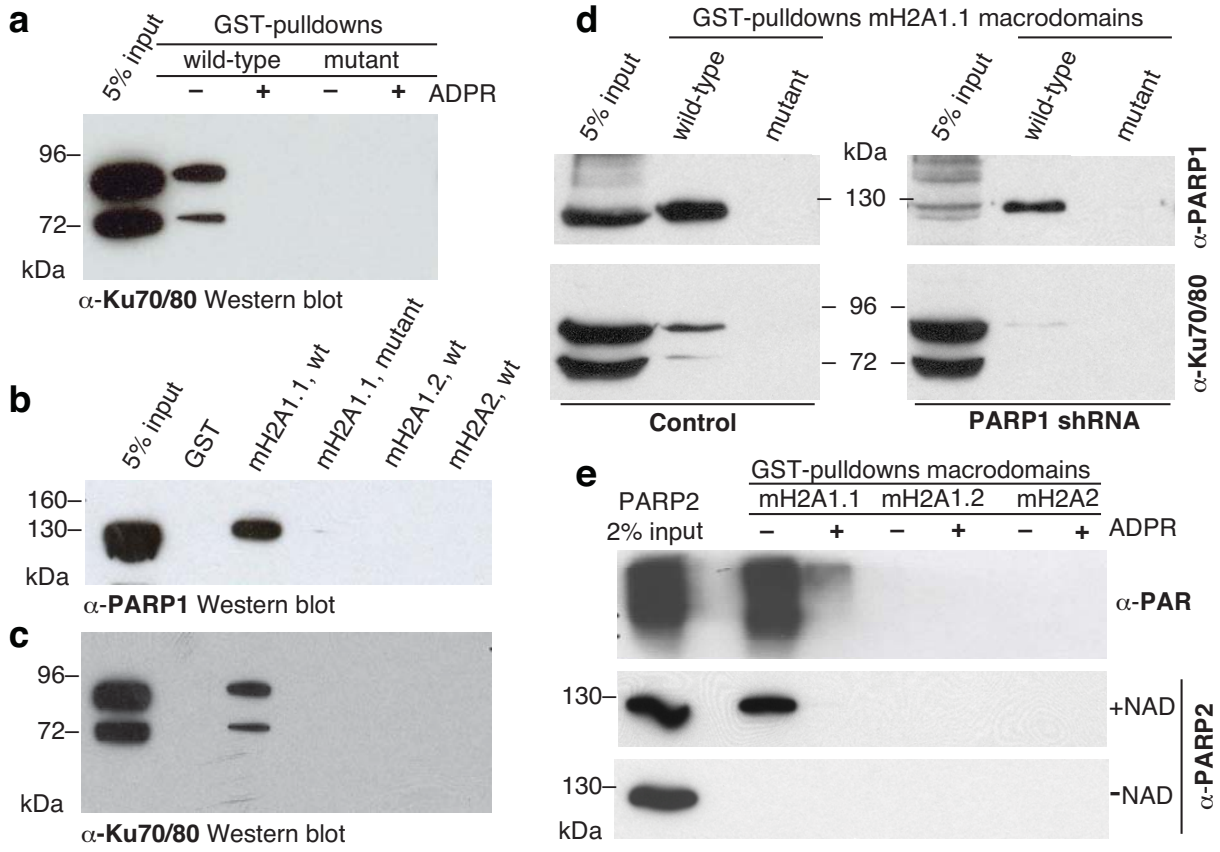

Supplementary Fig. 3 | Binding of Ku70/80 heterodimer to the macrodomain of histone macroH2A1.1 is mediated by PARylated PARP1.
a, Pulldown assay using GST-tagged macrodomains and HEK293 cell nuclear extracts. Ku70 and Ku 80 interact with wild-type (*wild-type*), but nc the double G224E/F351A point mutant (*mutant*). Free ADP-ribose in the wash buffer (ADPR) of the pulldown assay readily abolishes the inter between Ku proteins and the wild-type macroH2A1.1 macrodomain (WT). **b**, PARP1 interacts with the wild-type macroH2A1.1 macrod (*mH2A1.1, wt*), in contrast to mutant macroH2A1.1 (*mH2A1.1, mutant*), other macroH2A isoforms (*mH2A1.2, wt*; *mH2A2, wt*) or GST contr Ku70/80 interact with the wild-type macroH2A1.1 macrodomain (*mH2A1.1, wt*), in contrast to mutant macroH2A1.1 (*mH2A1.1, mutant*), macroH2A isoforms (*mH2A1.2, wt*; *mH2A2, wt*) or GST controls. **d**, Pulldown assay using GST-tagged macroH2A1.1 macrodomains in nuclear e from AGS cells treated with a short hairpin again PARP1. PARP1 knockdown cells show reduced levels of PARP1 protein (*5% input* lane; *right p* Nonetheless, PARP1 is efficiently pulled out by the macroH2A1.1 macrodomains under these knockdown conditions. Protein levels of Ku70/ unaffected in PARP1 RNAi cells, yet PARP1 knockdown decreases Ku70/80 binding to the macrodomains. **e**, Purified, recombinant PARP2 only to the macroH2A1.1 macrodomain when it has been incubated with NAD and free ADPR competes its interaction.

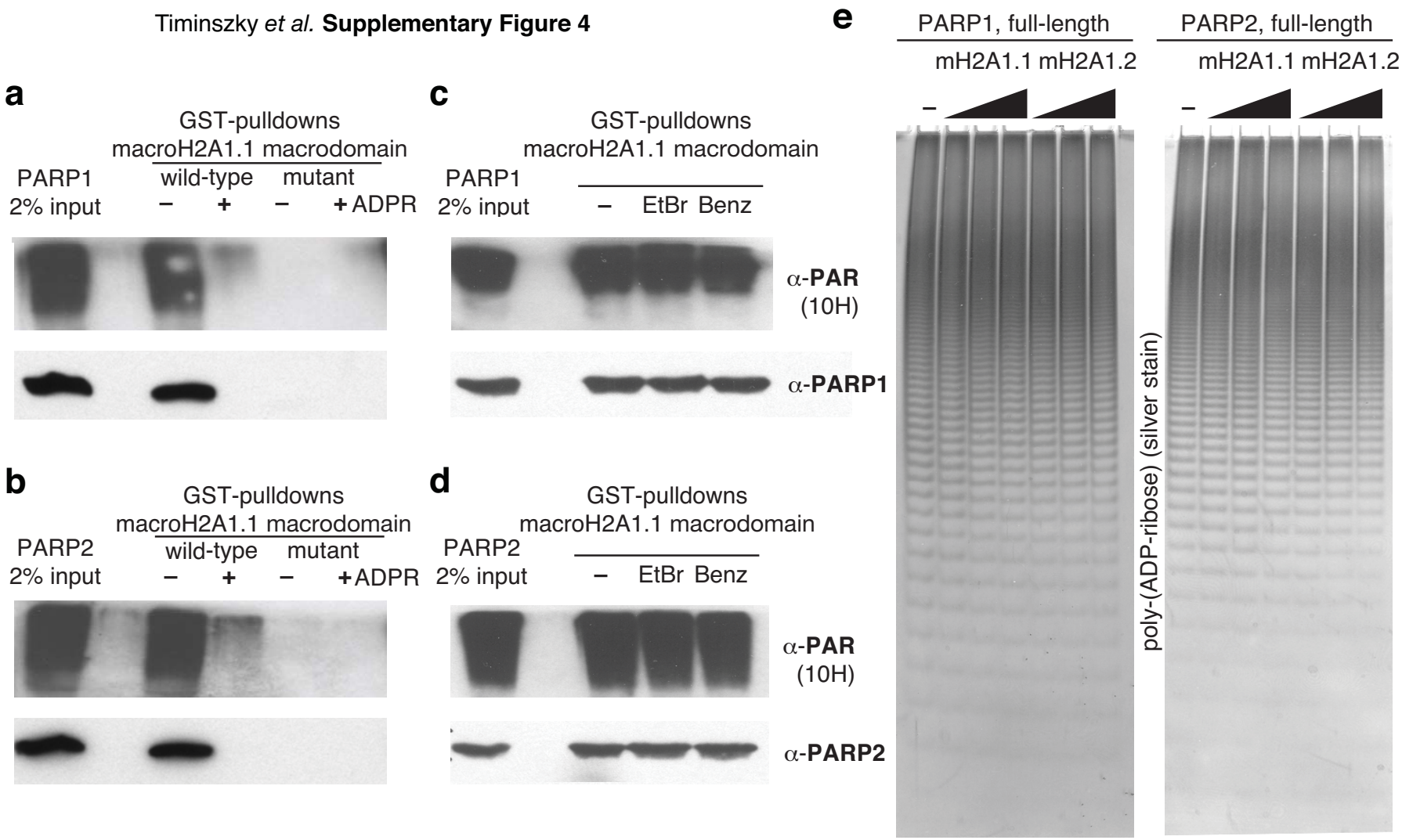

Supplementary Fig. 4 | The macroH2A1.1 macrodomain binds NAD-incubated, purified recombinant PARP1 and PARP2 directly. MacroH2A1.1/1.2 macrodomain do not inhibit PARP activity.

a-b, GST-pulldowns with NAD-treated purified, recombinant PARP1 (a) and PARP2 (b) reveals binding to the wild-type macroH2A1.1 macrodomain, but not to the ADPR-binding deficient G224E macroH2A1.1 point mutant. **c-d**, Addition of 100 μg/ml ethidium bromide (*EtBr*) or benzonase (*benz*) do not disrupt the interactions between the macroH2A1.1 macrodomains and NAD-treated, recombinant, immunopurified PARP1 (c) and PARP2 (d). **e**, Histone macrodomains do not affect PARP1 or PARP2 activity. PARP enzymes were activated and incubated with increasing amounts of macroH2A1.1 or macroH2A1.2 macrodomains (labeled *mH2A1.1* and *mH2A1.2*, respectively). PAR produced by PARP1 or PARP2 was then separated on an urea-PAGE gel and detected by silver staining. Contrary to a previous report with a macrodomain fragment or a construct containing the basic linker region between histone fold and macrodomain[9], our data show no effect of either macroH2A1.1 or macroH2A1.2 macrodomains on PARP1 or PARP2 enzymatic activity.

Timinszky *et al.* **Supplementary Figure 5**

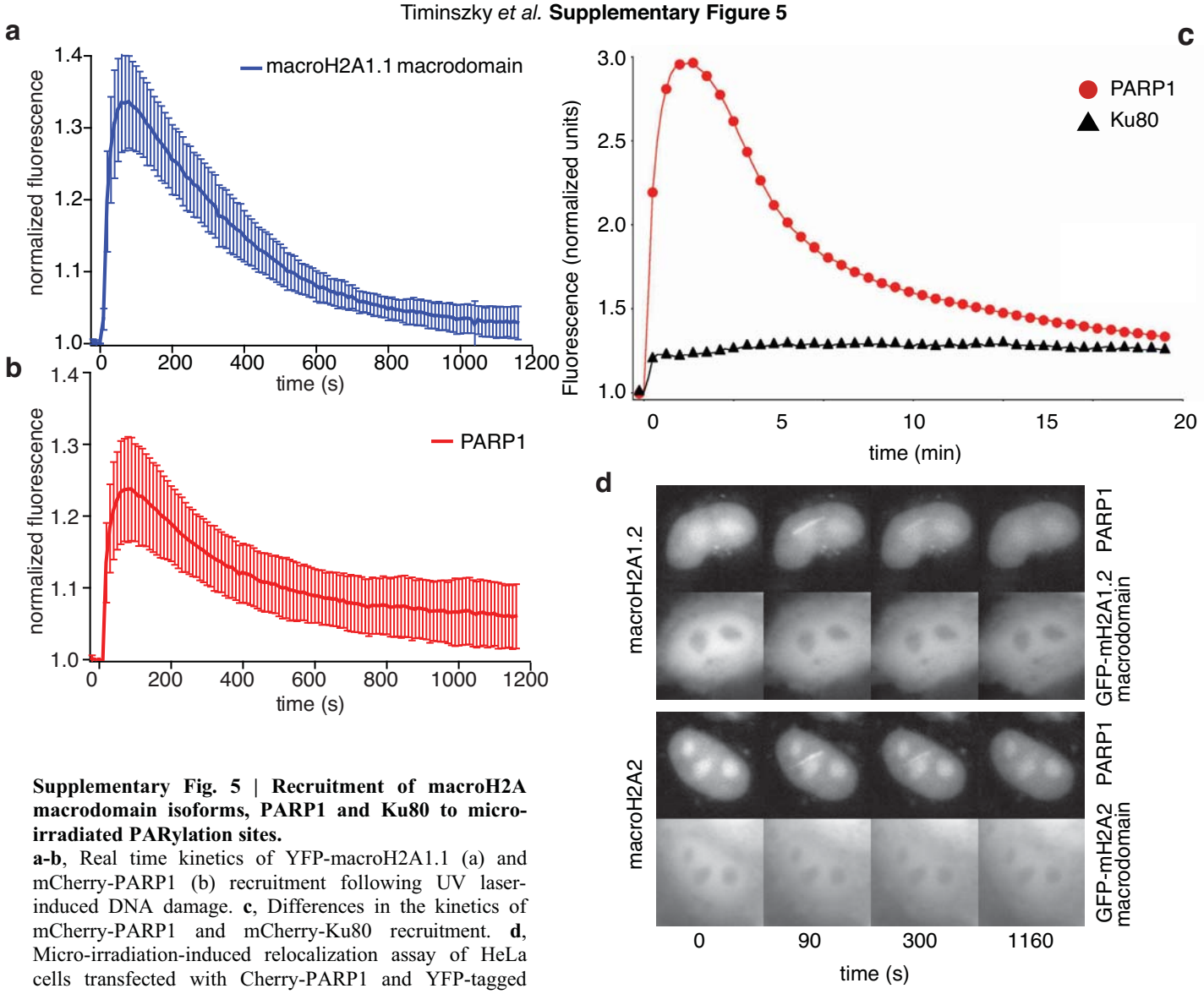

Supplementary Fig. 5 | Recruitment of macroH2A macrodomain isoforms, PARP1 and Ku80 to micro-irradiated PARylation sites.
a-b, Real time kinetics of YFP-macroH2A1.1 (a) and mCherry-PARP1 (b) recruitment following UV laser-induced DNA damage. **c**, Differences in the kinetics of mCherry-PARP1 and mCherry-Ku80 recruitment. **d**, Micro-irradiation-induced relocalization assay of HeLa cells transfected with Cherry-PARP1 and YFP-tagged macroH2A1.2 and macroH2A2 macrodomains.

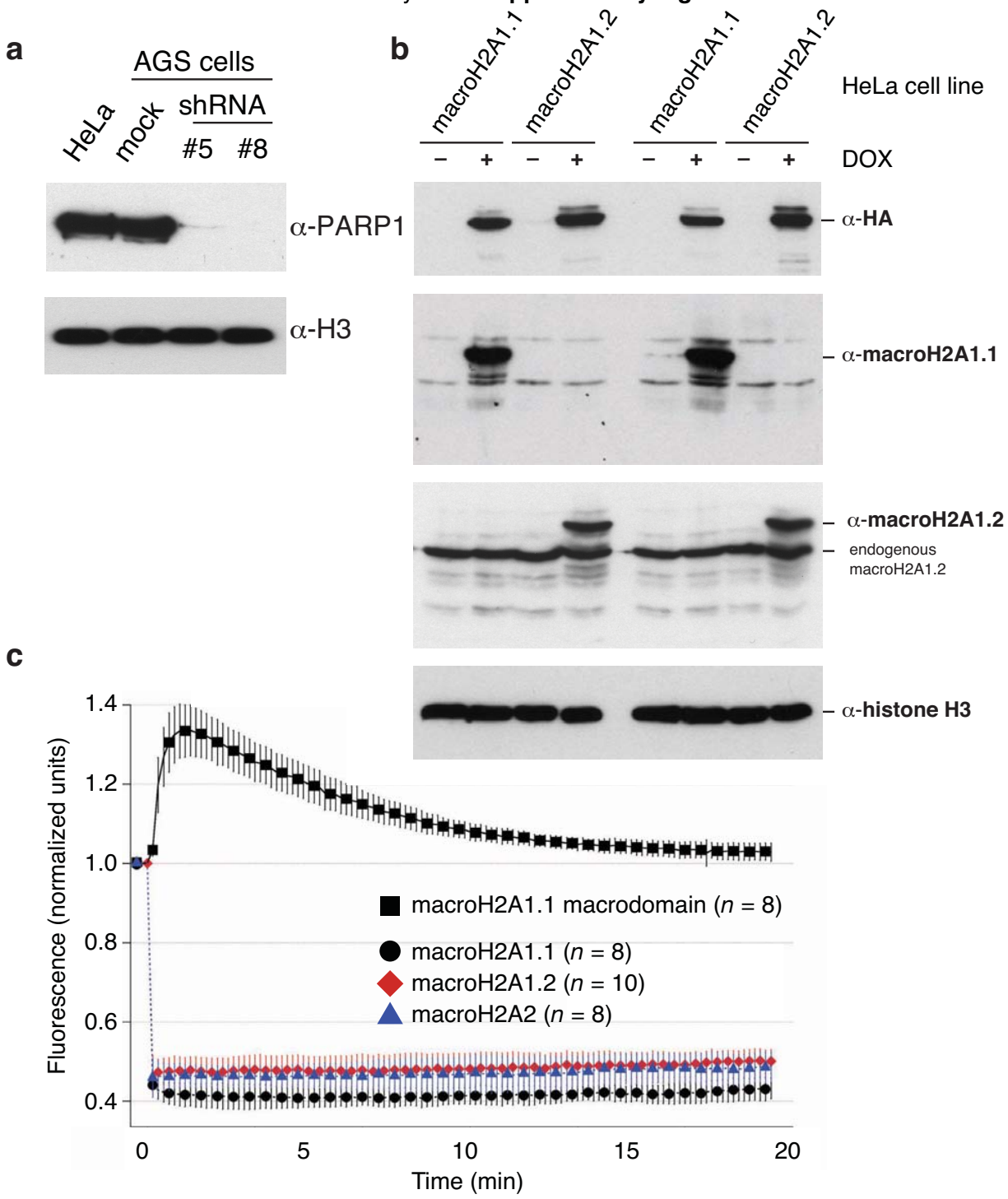

Supplementary Fig. 6 | PARP1 knockdown efficiency, macroH2A isoform transgene expression and FRAP imaging of 'immobile' nucleosomal macroH2A histones.
a, AGS cells treated with distinct short RNAi hairpins targeting PARP1 show reproducible levels of PARP1 knockdown (*left* and *right panels* correspond to two distinct biological samples). **b**, Western blots of macroH2A transgene expression in HeLa cell nuclei containing epitope-tagged macroH2A1.1 and macroH2A1.2 grown in the absence or presence of doxycycline using anti-HA, macroH2A1.1, macroH2A1.2 and H3 antibodies. MacroH2A1.2 IgG detect the abundant endogenous macroH2A1.2 protein . Addition of doxycycline reveals macroH2A1.1 and macroH2A1.2 transgene expression at levels comparable to those of endogenous macroH2A1.2. MacroH2A1.1 'over-expression' levels are similar to those of the endogenous amounts of its splice-variant isoform macroH2A1.2. **c**, FRAP assays comparing the recruitment kinetics for soluble YFP-macroH2A1.1 macrodomain at the DNA micro-irradiation site in comparison to the recovery of fluorescently-tagged full-length histones macroH2A1.1, macroH2A1.2 and macroH2A2 following DNA micro-irradiation.

Supplementary Fig. 7 | Timecourse of PAR-induced and macroH2A1.1-mediated chromatin rearrangement at laser micro-irradiated sites *in vivo*.
HeLa stable cell lines conditionally expressing macroH2A1.1 (**a-c**, **e**, **f)** or macroH2A1.2 (**d**) were induced (**a**, **b**, **d-f**) or not induced (**c**) with doxycycline and cultured overnight before laser micro-irradiation. Cells were fixed at the given times after laser micro-irradiation and immunostained with antibodies to HA for the FLAG-HA-tagged macroH2A1.1 or FLAG-HA-tagged macroH2A1.2 cell lines, antibodies to endogenous PARP1, endogenous histone H1, PAR or phosphorylated H2AX (γ-H2AX) and Hoechst staining (DNA). The micro-irradiated areas are identified by H2AX phosphorylation (**a**, **c**, **f**) or the recruitment of PARP1 (**b**, **d**, **e**). When the expression of macroH2A1.1 is induced and PARP1 enzymatic activity is not inhibited, chromatin rearranges and condenses at the site of laser micro-irradiation, as revealed by the increased signal of Hoechst, histone H1 or HA staining. The observed chromatin condensation is temporary and its lifetime correlates with the kinetics of PAR formation and breakdown. With increasing time after micro-irradiation, condensation in macroH2A1.1-expressing cells is observed in fewer cells and is undetectable by 25-30 minutes. Scale bar is 20 μm for main images and 10 μm for the inlays.

Nature Structural & Molecular Biology: doi:10.1038/nsmb.1664

MacroH2A1.1 expressed (Doxycycline added)

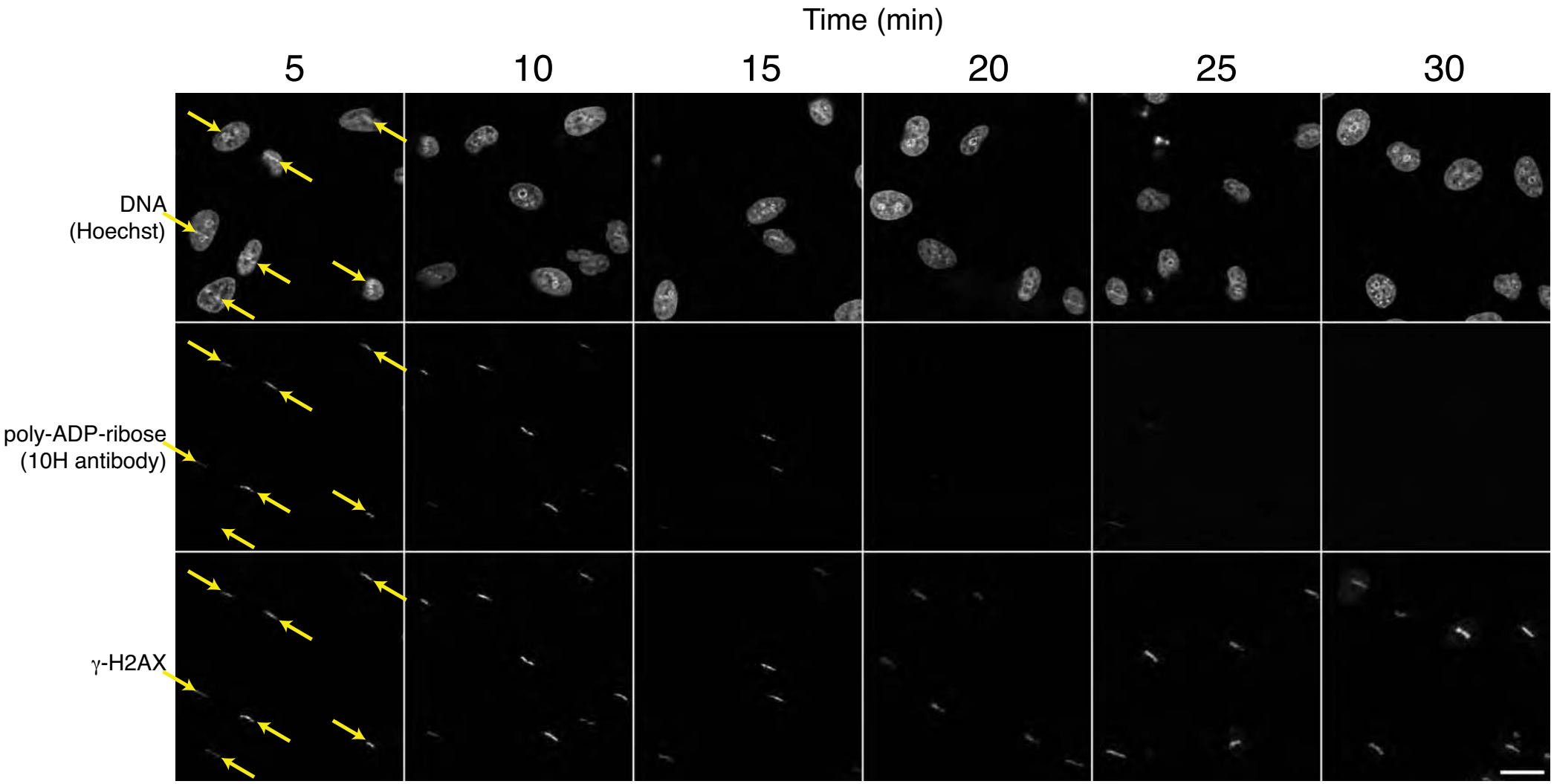

Scale bar is 20 μm.

Nature Structural & Molecular Biology: doi:10.1038/nsmb.1664

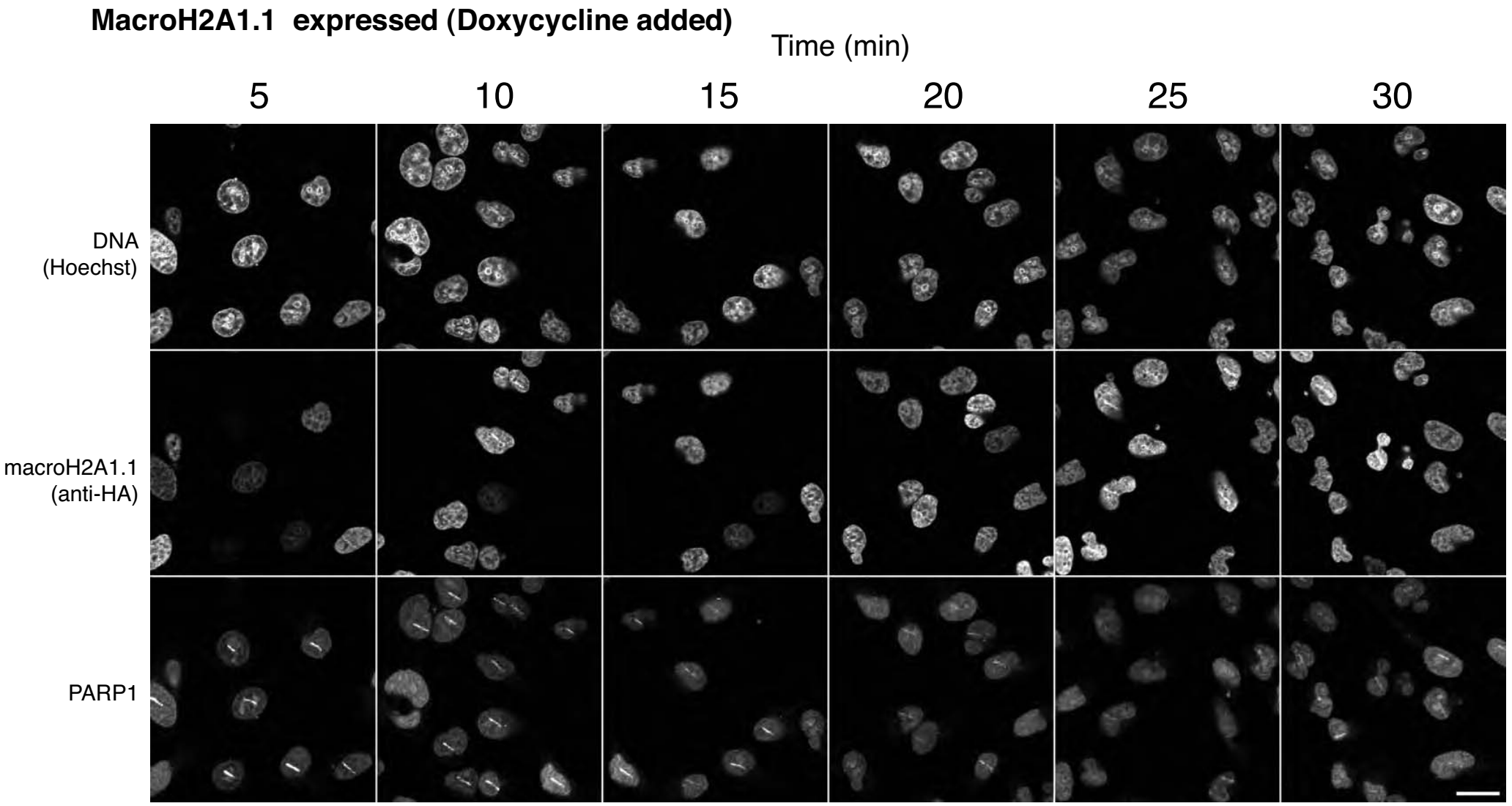

Scale bar is 20 μm.

No expression of macroH2A1.1 (without Doxycycline)

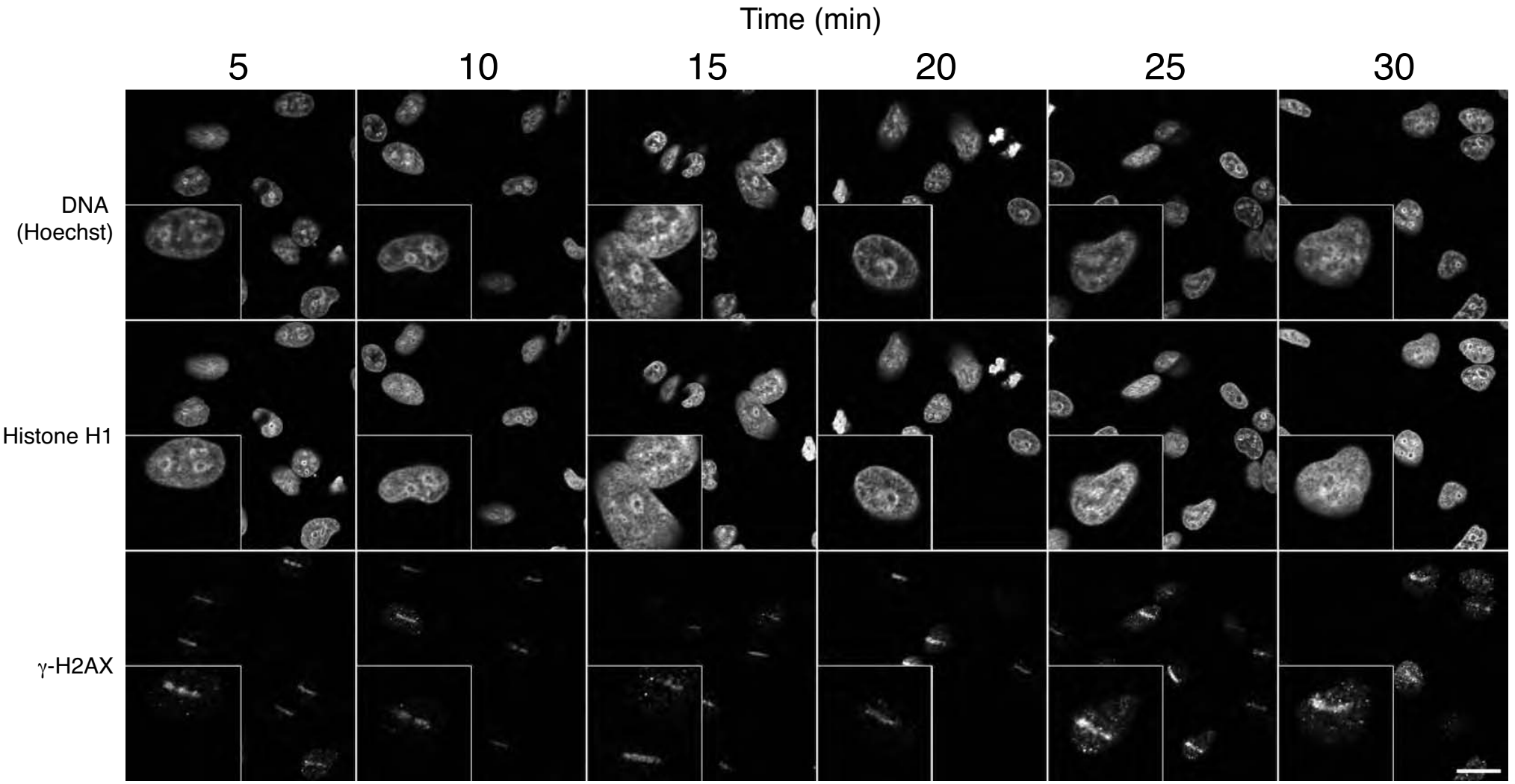

The scale bar is 20 μm in the main image and 10 μm in inlays.

MacroH2A1.2 expressed (Doxocycline added)

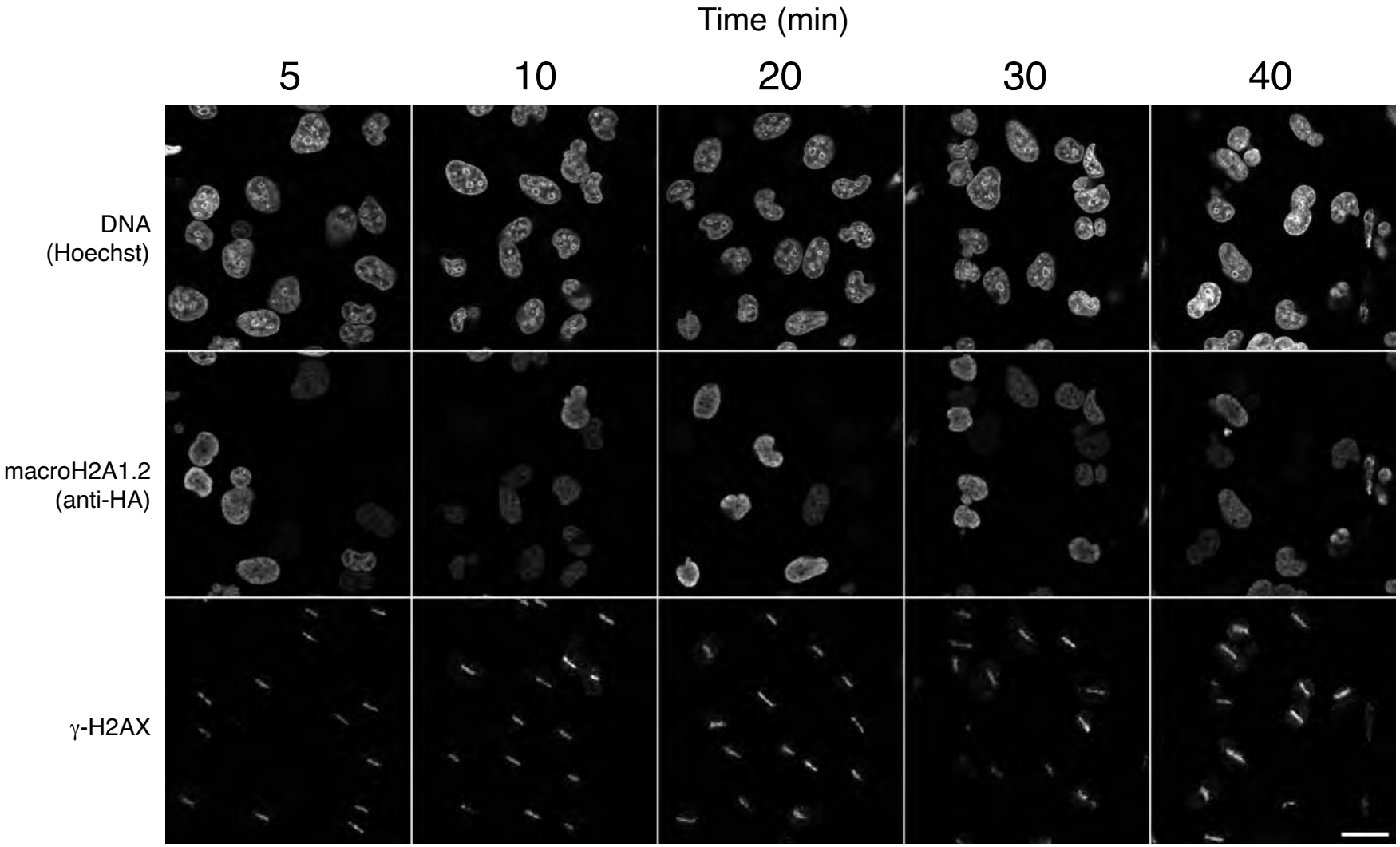

Scale bar is 20 μm.

Nature Structural & Molecular Biology: doi:10.1038/nsmb.1664

MacroH2A1.1 expressed, PARP inhibitor PJ-34 added

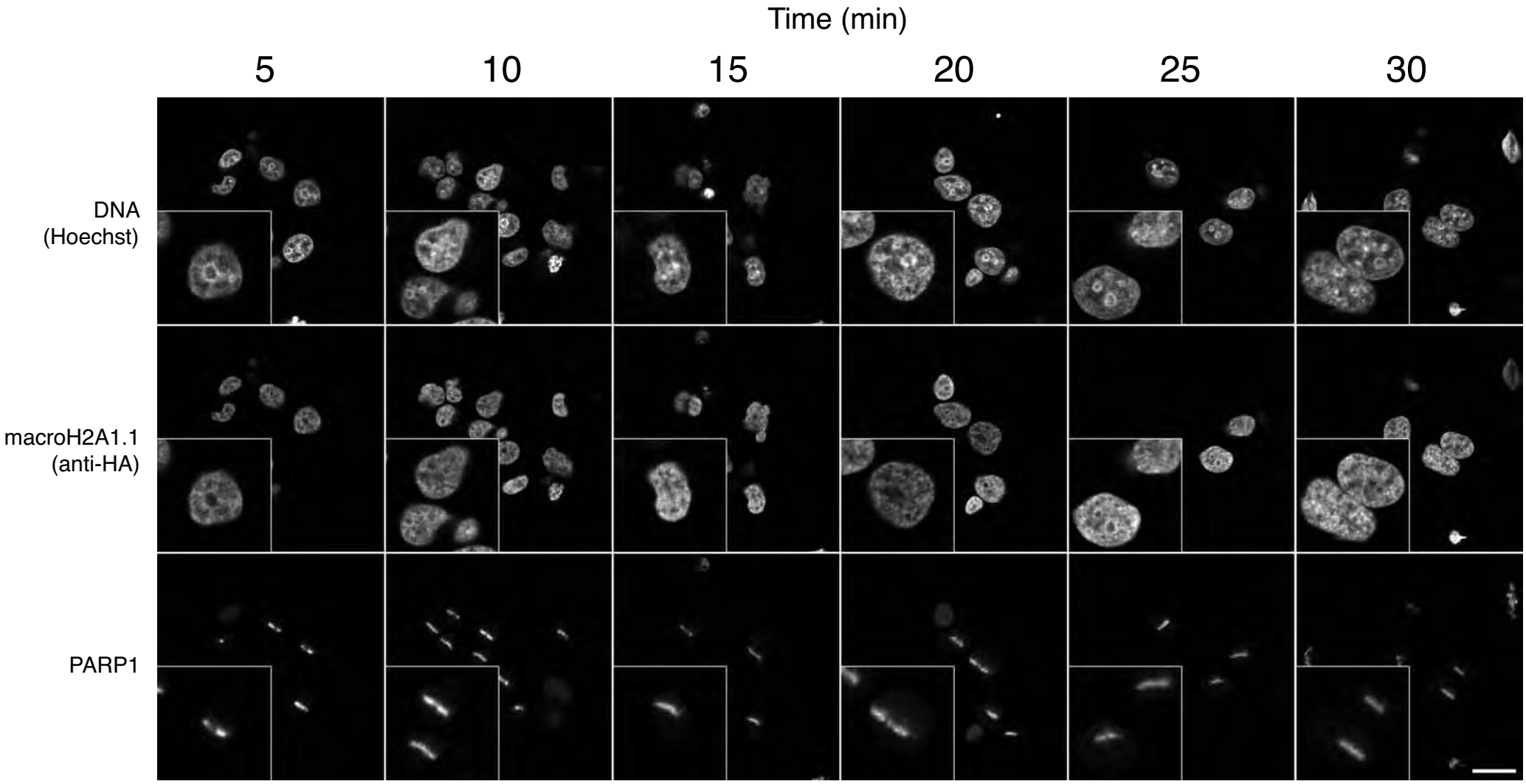

The scale bar is 20 μm in main image and 10 μm in inlays.

MacroH2A1.1 expressed (Doxycycline added)

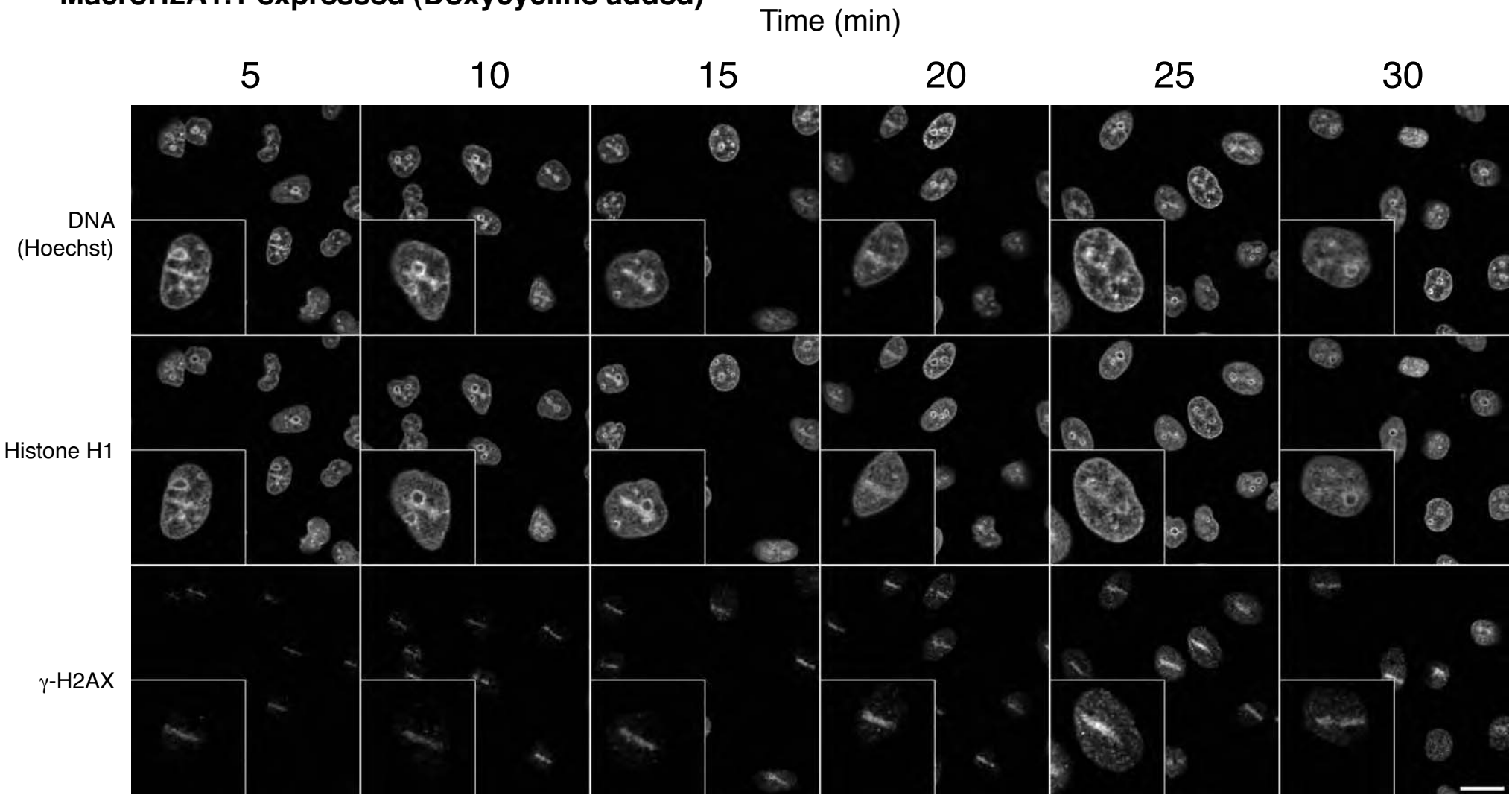

The scale bar equal 20 μm for main images and 10 μm for the inlays.

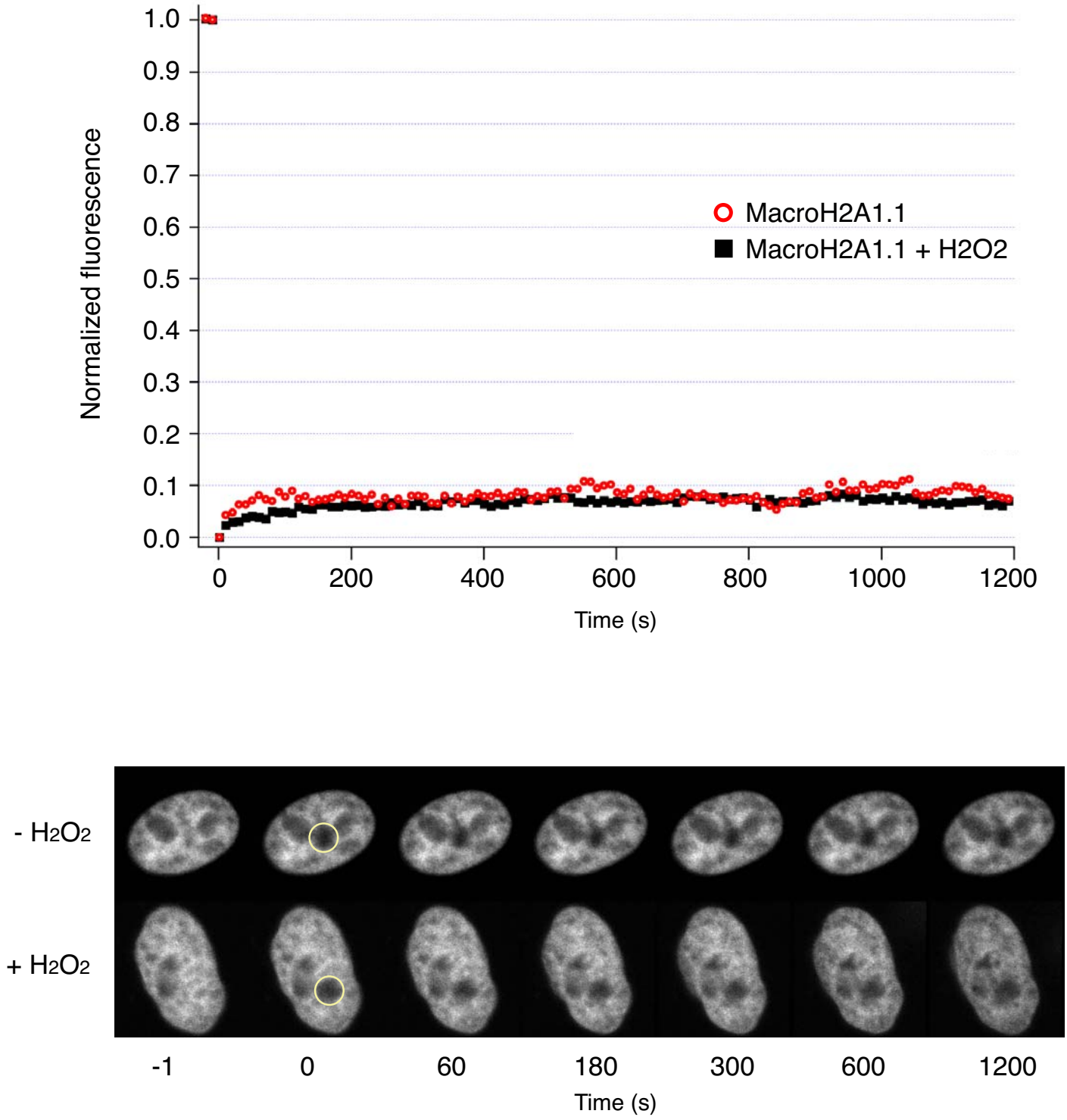

Supplementary Fig. 8 | FRAP assays of tagged macroH2A1.1 in the presence and absence of the DNA damage agent and PARP1 activator H_2O_2.
Fluorescently-tagged human macroH2A1.1 histone was bleached (yellow circle) and the recovery of the fluorescence signal at the bleached site was monitored over 20 minutes.

Timinszky *et al.* **Supplementary Figure 9**

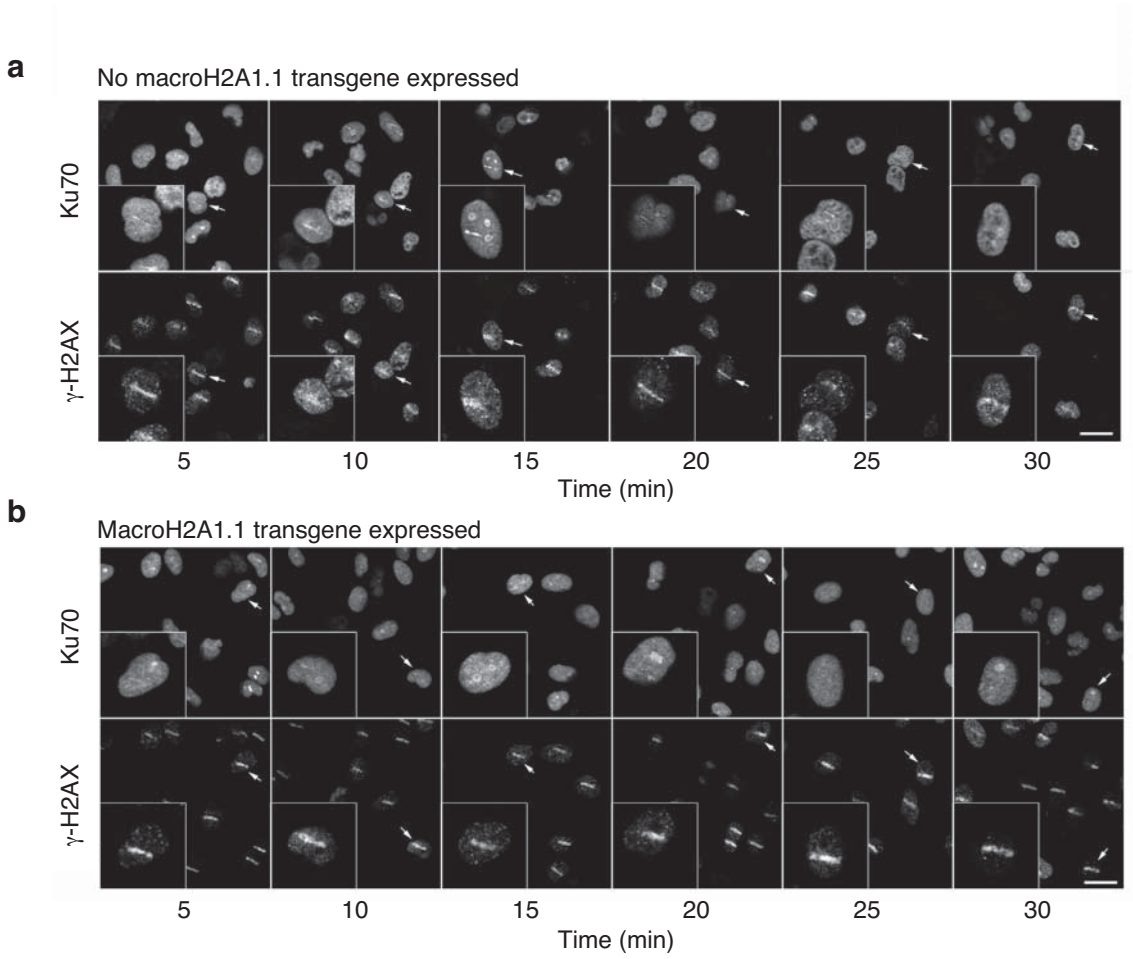

Supplementary Fig. 9

MacroH2A1.1 expression reduces recruitment of cellular Ku80 to DNA damage sites.

Immunofluorescence staining with Ku70 and !-H2AX antibodies in human TetOn HeLa cells either expressing (*doxycycline-induced*) or not expressing (*uninduced*) the tagged macroH2A1.1 histone isoform.

Timecourse analysis and insets reveal a reduction in the recruitment of Ku70 upon DNA micro-irradiation in cells that contain macroH2A1.1. Scale bar is 20 μm for main images and 10 μm for the inlays.

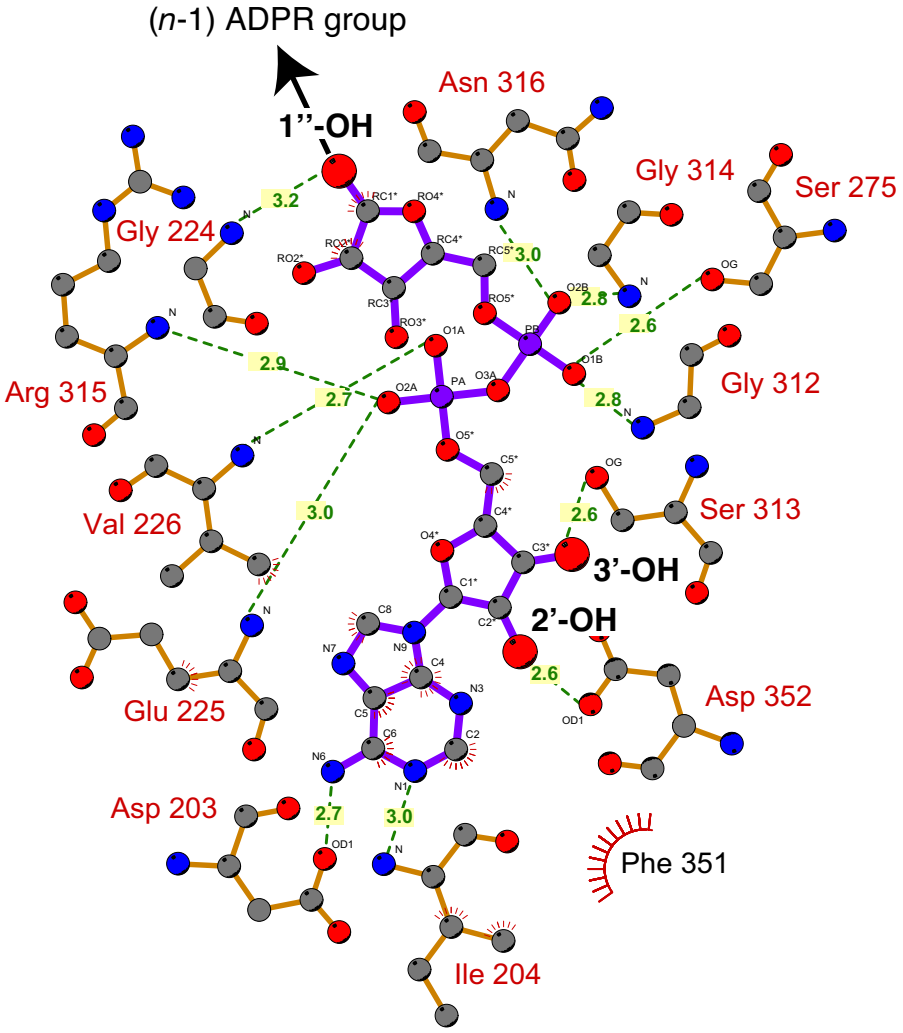

Supplementary Fig. 10 | Schematic representation of ADP-ribose binding to the macrodomain of histone macroH2A1.1.
The *LigPlot* diagram summarizes key interactions between the ADPR ligand and macrodomain binding pocket residues. Legend: *purple lines*, ADP-ribose; *orange lines*, MacroH2A1.1 residues; *semicircles with radiating lines*; atoms or residues involved in hydrophobic contacts between protein and ligand. The capped 2' and 3'-OH groups in the proximal ribose and the accessible 1"-OH group in the distal ribose are highlighted by using larger red balls as symbols.

Protein name	Sequence coverage (%)	Description
macroH2A1.2	37.5	Bait
H4 H2A H2B H3	36.4	Core histones
DNA-PKcs Ku80 Ku70	24.5	Core machinery for NHEJ; Functions in DNA repair and V(D)J recombination.
SSRP1 Spt16	16.0	FACT complex. Transcription, replication, silencing, etc.
14-3-3 zeta	9.8	Phosphoserine binding protein
hnRNP A2/B1 hnRNP A1 B	9.4	hnRNPs
PP2Cγ	7.3	Alternative splicing and histone assembly
Topo IIa Topo I	7.2	Topoisomerases
H1.4	6.9	Linker histone
PHF-14	6.0	Uncharacterized PHD finger protein
Importin 9	6.0	Imports histones and other proteins
Mi-2-α MTA1 MTA2 RpAb48 HDAC2 p66α	5.7	NuRD complex Histone deacetylase, chromatin remodeling gene silencing.
Hsp90ß	5.6	Heat shock protein
DEK	5.1	Transcription factor and/or architectual protein.
Snf2h Rsf-1	4.8	RSF complex. Nucleosome assembly and spacing.
PARP-1	4.7	Poly(ADP-ribose) Polymerase
$p14^{ARF}$	4.5	Cell cycle control; senescence

Supplementary Table 1 | Mass spectrometry (MS) analysis.

HA-antibody mediated purification of Flag-PreScissionProtease-HA-tagged macroH2A1.2 in nuclear extracts from HeLa cells reveal holo-DNA-PK complex (consisting of the catalytic DNA-dependent protein kinase subunit and the ATP-dependent DNA helicases Ku70 and Ku80), PARP1, core histones, the histone chaperones FACT and PP2Cγ, the repressive NURD complex and several other proteins as biochemical interactors of tagged, cellular macroH2A1.2.

	MASCOT Score	Sequence coverage
DNA-PKcs	508	24%
PARP1	304	50%
Ku80	204	50%
Ku70	92	32%

Supplementary Table 2 MS identification of 4 proteins in human nuclear extracts that specifically associate with wild-type, but not an ADP-ribose-binding-deficient macrodomain of the human histone variant macroH2A1.1.